Submitted to Physical Review

LBL-1104
Preprint

FREQUENCY AND WAVEVECTOR DEPENDENT DIELECTRIC FUNCTION FOR Ge, GaAs, AND ZnSe

S. J. Sramek and Marvin L. Cohen

July 1972

AEC Contract No. W-7405-eng-48

For Reference

Not to be taken from this room

LBL-1104

DISCLAIMER

This document was prepared as an account of work sponsored by the United States Government. While this document is believed to contain correct information, neither the United States Government nor any agency thereof, nor the Regents of the University of California, nor any of their employees, makes any warranty, express or implied, or assumes any legal responsibility for the accuracy, completeness, or usefulness of any information, apparatus, product, or process disclosed, or represents that its use would not infringe privately owned rights. Reference herein to any specific commercial product, process, or service by its trade name, trademark, manufacturer, or otherwise, does not necessarily constitute or imply its endorsement, recommendation, or favoring by the United States Government or any agency thereof, or the Regents of the University of California. The views and opinions of authors expressed herein do not necessarily state or reflect those of the United States Government or any agency thereof or the Regents of the University of California.

0 0 0 0 3 8 0 4 0 1 2

LBL-1104

Frequency and Wavevector Dependent Dielectric Function for Ge, GaAs, and ZnSe.*

S. J. Sramek and Marvin L. Cohen

Department of Physics, University of California

and

Inorganic Materials Research Division, Lawrence Berkeley Laboratory

Berkeley, California 94720

Abstract

The frequency and wavevector dependent dielectric function for Ge, GaAs, and ZnSe is calculated from the electronic band structures obtained by the Empirical Pseudopotential Method. The results show the effect of increasing ionicity on the dielectric function. The results also yield the plasmon dispersion relation $\omega(q)$ for the three semiconductors. The frequency and wavevector dependent Penn dielectric function is calculated and compared with the results for Ge.

*Research supported in part by the National Science Foundation Grant GP 13632.

I. Introduction. We have calculated[1] the frequency and wavevector dependent dielectric function $\epsilon(\underset{\sim}{q},\omega)$ in the [100] direction for Ge, GaAs, and ZnSe. This dielectric function describes the screening of a longitudinal field which varies in both space and time. This is the first calculation of $\epsilon(\underset{\sim}{q},\omega)$ for these materials using realistic energy bands and wavefunctions. These three crystals were chosen to observe the changes in $\epsilon(\underset{\sim}{q},\omega)$ as one moves through a series from a completely covalent compound (Ge) to compounds with decreasing covalency (GaAs and ZnSe).

The present calculations of $\epsilon(\underset{\sim}{q},\omega)$ are similar to that done by Walter and Cohen[2] for Si. The real part of the dielectric function, $\epsilon_1(\underset{\sim}{q},\omega)$, is calculated directly, and the imaginary part, $\epsilon_2(\underset{\sim}{q},\omega)$, is calculated using the Kramers-Kronig transformation. The details and results of the calculation are given in Sec. II. In Sec. III the results for Ge are compared with a calculation of $\epsilon_1(\underset{\sim}{q},\omega)$ using the Penn model.[3]

II. Calculations and Results. First we calculate the longitudinal wavevector and frequency dependent dielectric function $\epsilon(\underset{\sim}{q},\omega)$ which describes the crystal response to an electric field parallel to $\underset{\sim}{q}$ and varying sinusoidally in time:

$$\underset{\sim}{D}\, e^{i(\underset{\sim}{q}\cdot\underset{\sim}{r} - \omega t)} = \epsilon(\underset{\sim}{q},\omega)\,\underset{\sim}{E}\, e^{i(\underset{\sim}{q}\cdot\underset{\sim}{r} - \omega t)} \,. \tag{2.1}$$

Using the result for ϵ_1 obtained by Ehrenreich and Cohen,[4] we obtain

$$\epsilon_1(\underset{\sim}{q},\omega) = 1 + \frac{4\pi e^2}{\Omega q^2} \sum_{\underset{\sim}{k},c,v}{}' \left|\langle \underset{\sim}{k},c \,|\, \underset{\sim}{k}+\underset{\sim}{q},v\rangle\right|^2 \tag{2.2}$$

$$\times \left\{ \left[E_c(\underset{\sim}{k}) - E_v(\underset{\sim}{k}+\underset{\sim}{q}) - \hbar\omega\right]^{-1} + \left[E_c(\underset{\sim}{k}) - E_v(\underset{\sim}{k}+\underset{\sim}{q}) + \hbar\omega\right]^{-1} \right\} \,.$$

The matrix element is the inner product between the periodic parts of the Bloch functions, $\underset{\sim}{k}$ is summed over the first Brillouin zone, v labels the valence bands, and c labels the conduction bands. For computational purposes Eq. (2.2) is rewritten as

$$\epsilon_1(\underset{\sim}{q},\omega) = 1 + \frac{4\pi e^2}{q^2}\,\frac{2}{(2\pi)^3}\sum_{\underset{\sim}{k},c,v} |\langle \underset{\sim}{k}, c\,|\,\underset{\sim}{k}+\underset{\sim}{q}, v\rangle|^2\,(\Delta k)^3$$
$$\times \{[E_c(\underset{\sim}{k}) - E_v(\underset{\sim}{k}+\underset{\sim}{q}) - \hbar\omega]^{-1} + [E_c(\underset{\sim}{k}) - E_v(\underset{\sim}{k}+\underset{\sim}{q}) + \hbar\omega]^{-1}\}\ , \tag{2.3}$$

where the summation is over a grid of 3360 points in the Brillouin zone. $(\Delta k)^3$ is the volume of a cube associated with each point, with suitable truncations at the zone boundaries. The coordinates of the calculated points are given by $\frac{1}{16}(2s+1,\ 2m+1,\ 2n+1)$ in units of $2\pi/a$, where s, m, n are integers. The indices v and c span the top four valence bands and the bottom eleven conduction bands. The wavefunctions and energies are obtained by the empirical pseudopotential method,[5] using the pseudopotential form factors of Cohen and Bergstresser.[6] Spin-orbit interactions were not included in this calculation.

The dielectric function cannot be calculated for an arbitrary $\underset{\sim}{q}$ because of computer time limitations. Crystal symmetry can be exploited to considerably reduce the time if $\underset{\sim}{q}$ is restricted to the [100] direction. In addition, $|\underset{\sim}{q}|$ must be restricted to the values $\frac{1}{8}n$, in units of $2\pi/a$, where n is an integer, so that $\underset{\sim}{k}+\underset{\sim}{q}$ also lies on the grid of calculated points.

The term $[E_c(\underset{\sim}{k}) - E_v(\underset{\sim}{k}+\underset{\sim}{q}) - \hbar\omega]^{-1}$ in Eq. (2.3) can have singularities at some points in the Brillouin zone. If the cube of volume $(\Delta k)^3$ contains such points, then the energy values at the cube center cannot accurately

represent $(E_c - E_v - \hbar\omega)^{-1}$ over the entire cube. For such cases, the large cube is divided into 216 equal sub-cubes, and the energies E_c and E_v are calculated for each sub-cube by interpolation.

After calculating $\epsilon_1(q,\omega)$, we calculate the imaginary part $\epsilon_2(q,\omega)$ by a Kramers-Kronig transform of $\epsilon_1(q,\omega)$. Figs. 1-6 display three-dimensional perspective plots of $\epsilon_1(q,\omega)$ and $\epsilon_2(q,\omega)$ for the three semiconductors. Each curve represents ϵ_1 or ϵ_2 as a function of ω for fixed q. The q values are $q = 1/4$, $1/2$, $3/4$, and 1 in units of $2\pi/a$ in the [100] direction. The dielectric functions were also calculated for $q = 1/8$, $3/8$, $1\frac{1}{4}$, $1\frac{1}{2}$, and 2, but those results are not plotted.

By considering the points (q,ω) for which the calculated $\epsilon_1 = 0$, and by fitting a curve through these points, we obtain for each material two curves in the (q,ω) plane along which $\epsilon_1(q,\omega) = 0$, which we denote by $\omega_t(q)$ and $\omega_\ell(q)$. The results are plotted in Fig. 7. From Eq. (2.1) we see that, if $\epsilon(q,\omega) = 0$, then a nonzero electric field can exist in the material even if no field is applied externally; i.e. a plasmon can be present. For the three materials considered here, the lower zero $\omega_t(q)$ does not represent a physically observable plasmon mode, because, as can be seen in Figs. 1-6, both ϵ_1 and ϵ_2 are always near their largest values when near $\omega_t(q)$; i.e. $\omega_t(q)$ resembles a damped pole in ϵ_1.

As we move through the series from completely covalent Ge through somewhat ionic GaAs to the higher ionicity compound, ZnSe, we observe three important qualitative features of ϵ_1:

1) The higher zeroes of ϵ_1, representing the plasmon mode $\omega_\ell(q)$, change very little.

2) The lower zeroes of ϵ_1, $\omega_t(q)$, increase substantially.

3) The $\omega = 0$ values and the peak values of ϵ_1 decrease substantially.

The reasons for these effects may be understood by examining Eq. (2.2).

Because Ge, GaAs, and ZnSe all have almost exactly the same lattice constant and are composed of elements all from the same row of the periodic table, they all have almost exactly the same symmetric pseudopotential. The principal change in moving through the series is that an antisymmetric pseudopotential is introduced and becomes larger. For a given $(\underset{\sim}{k},c,v)$ the energy difference $E_c(\underset{\sim}{k}) - E_v(\underset{\sim}{k}+\underset{\sim}{q})$ tends to become <u>larger</u>. Assuming that changes in the matrix elements in Eq. (2.2) are not important, we may conclude the following:

1) At high frequencies, $\hbar\omega >> (E_c - E_v)$ for all band pairs (c,v) for which the matrix elements are not small. Then $(E_c - E_v - \hbar\omega)^{-1} + (E_c - E_v + \hbar\omega)^{-1} \rightarrow 2(E_c - E_v)/(\hbar\omega)^2$, and we expect $\epsilon_1(q,\omega)$ at high frequencies to be only weakly dependent on the energy differences $(E_c - E_v)$. The true plasmon mode $\omega_\ell(q)$ should therefore be little affected by the antisymmetric pseudopotential and in fact is not far from the free electron value (e.g., 15.6 eV for Ge).

2) For small frequencies, $\hbar\omega < (E_c - E_v)$ for all (k,c,v); as $\hbar\omega$ increases, $(E_c - E_v - \hbar\omega)^{-1}$ at first increases rapidly so that all terms in the sum over $(\underset{\sim}{k},c,v)$ increase rapidly. $\epsilon_1(q,\omega)$ reaches a peak and begins

decreasing when $\hbar\omega$ passes the smallest of the energy differences $(E_c - E_v)$, so that some of the terms $(E_c - E_v - \hbar\omega)^{-1}$ suddenly become large and negative. $\epsilon_1(q,\omega)$ passes through zero when so many of the terms $(E_c - E_v - \hbar\omega)^{-1}$ have become negative that they balance the positive terms in the sum over $(\underset{\sim}{k}, c, v)$. This occurs when $\hbar\omega$ becomes roughly equal to an "average energy gap" between the top valence and the bottom conduction bands. This value is probably connected with the Phillips average gap.[7] When the antisymmetric pseudopotential is introduced and the energy differences $(E_c - E_v)$ become larger, the frequency $\hbar\omega$ at which the negative terms $(E_c - E_v - \hbar\omega)^{-1}$ balance the positive terms in the sum over $(\underset{\sim}{k}, c, v)$ must also become larger. The lower zero $\omega_t(q)$ should therefore increase.

3) At zero frequency, Eq. (2.2) becomes

$$\epsilon_1(q,\omega = 0) = 1 + \frac{8\pi e^2}{\Omega q^2} \sum_{\underset{\sim}{k}, c, v} |\langle \underset{\sim}{k}, c | \underset{\sim}{k+q}, v \rangle|^2 \{E_c(\underset{\sim}{k}) - E_v(\underset{\sim}{k+q})\}^{-1} .$$

Since the antisymmetric pseudopotential causes the energy differences $(E_c - E_v)$ to increase, all terms in the sum decrease. The static and low-frequency values of ϵ_1 should therefore decrease.

III. The Penn Model. We have calculated the Penn model dielectric function for comparison with our Ge results. This model makes the assumptions:

1) There is no Brillouin zone.

2) The energy $E(\underset{\sim}{k})$ is spherically symmetric, with a step discontinuity of magnitude E_g at the fermi surface.

3) The eigenfunction of wavevector $\underset{\sim}{k}$ is a superposition of just two plane waves, of wavevectors $\underset{\sim}{k}$ and $\underset{\sim}{k} - 2k_F\hat{k}$. Based on these assumptions, one

0 0 0 0 3 8 0 4 3 1 3

can set up and solve a simple 2×2 secular equation and obtain analytic expressions for $E(\underset{\sim}{k})$ and for the eigenfunctions. These expressions are given by Penn.[3] The dielectric function of this electron gas can then be calculated as a sum similar to (2.2).

In previous zero-frequency calculations,[3,8] to avoid the use of computing machines, Penn's expressions for $E(\underset{\sim}{k})$ and for the matrix elements in (2.2) were replaced with simplified expressions. In particular, $E(\underset{\sim}{k})$ was assumed parabolic (i.e. free electron-like) everywhere except in a region near the fermi surface; there, $E(\underset{\sim}{k})$ is assumed equal to $E_F \pm \frac{1}{2}E_g$ (+ for $k > k_F$, - for $k < k_F$), so that the "bands" are perfectly flat in a region near the fermi surface, with an energy gap E_g.

One can easily show that this "flat band" simplification will cause $\epsilon_1(q,\omega)$ to exhibit a first order pole <u>exactly</u> at $\hbar\omega = E_g$ for all $q < 2k_F$. Because the lower zero of the Ge $\epsilon_1(q,\omega)$ increases significantly with q (Fig. 7), we expect that the Penn model with the flat band simplification cannot closely approximate the calculated $\epsilon_1(q,\omega)$ for Ge.

Accordingly, we have numerically computed the Penn dielectric function using the exact $E(\underset{\sim}{k})$ and eigenfunctions proposed by Penn. We chose $E_g = 4.3$ electron volts, the principal optical gap of Ge, and k_F so that the associated electron concentration is equal to the Ge valence electron concentration. The results are plotted in Figs. 8 and 9.

The Penn model $\epsilon_1(q,\omega = 0)$ agrees fairly well with the result of Walter and Cohen[9] (identical to our result) for Ge. The numbers are given in Table I. However, for intermediate and high frequencies the agreement is poor. The Penn model polarizability at higher frequencies is considerably larger than

the calculated Ge polarizability based on the Ge $E(\underset{\sim}{k})$. As a result, the upper zeroes of $\epsilon_1(q,\omega)$ occur at appreciably higher frequencies than in the Ge case.

This low frequency agreement and high frequency disagreement may be understood as follows. The dielectric function for zero frequency is of the form

$$\epsilon_1(q,\omega = 0) = 1 + \frac{1}{q^2} \sum \frac{M^2}{E_{\underset{\sim}{k}+\underset{\sim}{q}} - E_{\underset{\sim}{k}}} ,$$

whereas for high frequencies

$$\epsilon_1(q,\omega \to \infty) = 1 - \frac{1}{(\hbar\omega)^2} \cdot \frac{1}{q^2} \sum M^2(E_{\underset{\sim}{k}+\underset{\sim}{q}} - E_{\underset{\sim}{k}}) .$$

So, for low frequencies the polarizability involves the ratios of matrix elements and energy differences; whereas, for high frequencies it involves the products of matrix elements and energy differences. We suggest that both the energy differences $E_{\underset{\sim}{k}+\underset{\sim}{q}} - E_{\underset{\sim}{k}}$ and the valence-conduction coupling matrix elements M^2 tend to be larger for the Penn model than for true Ge. If so, then the high frequency Penn model polarizability, involving the products $M^2(E_{\underset{\sim}{k}+\underset{\sim}{q}} - E_{\underset{\sim}{k}})$, should be considerably larger than the values for Ge, whereas the low frequency polarizability, involving the ratios $M^2/(E_{\underset{\sim}{k}+\underset{\sim}{q}} - E_{\underset{\sim}{k}})$, may not be substantially different from the Ge case.

Acknowledgement

Part of this work was done under the auspices of the U. S. Atomic Energy Commission. We would like to thank Professor John Walter for his help with the computer programming.

0 0 0 0 3 8 0 4 3 1 4

References

1. A preliminary account of the results of the present work was given in S. J. Sramek and M. L. Cohen, Bull. A. P. S. 17, 26 (1972).
2. John Walter and M. L. Cohen, Phys. Rev. B5, 3101 (1972).
3. D. R. Penn, Phys. Rev. 128, 2093 (1962).
4. H. Ehrenreich and M. H. Cohen, Phys. Rev. 115, 786 (1959).
5. M. L. Cohen and V. Heine, Solid State Physics 24, 37 (1971).
6. M. L. Cohen and T.K. Bergstresser, Phys. Rev. 141, 789 (1966).
7. J. C. Phillips, Rev. Modern Phys. 42, 317 (1970).
8. G. Srinivasan, Phys. Rev. 178, 1244 (1969).
9. John Walter and M. L. Cohen, Phys. Rev. B2, 1821 (1970).

Figure Captions

Fig. 1. $\epsilon_1(q,\omega)$ for Ge.

Fig. 2. $\epsilon_1(q,\omega)$ for GaAs.

Fig. 3. $\epsilon_1(q,\omega)$ for ZnSe.

Fig. 4. $\epsilon_2(q,\omega)$ for Ge.

Fig. 5. $\epsilon_2(q,\omega)$ for GaAs.

Fig. 6. $\epsilon_2(q,\omega)$ for ZnSe.

Fig. 7. Zeroes of $\epsilon_1(q,\omega)$ for Ge, GaAs, and ZnSe.

Fig. 8. $\epsilon_1(q,\omega)$ for the Penn model.

Fig. 9. $\epsilon_2(q,\omega)$ for the Penn model.

Table I

$q\left(\frac{2\pi}{a}\right)$	$\epsilon_1(q,\omega = 0)$	
	Walter and Cohen	Penn model
0.125	12.7	14.8
0.250	10.3	10.5
0.375	8.0	7.5
0.500	6.2	5.7
0.750	4.0	4.0
1.000	2.8	3.5

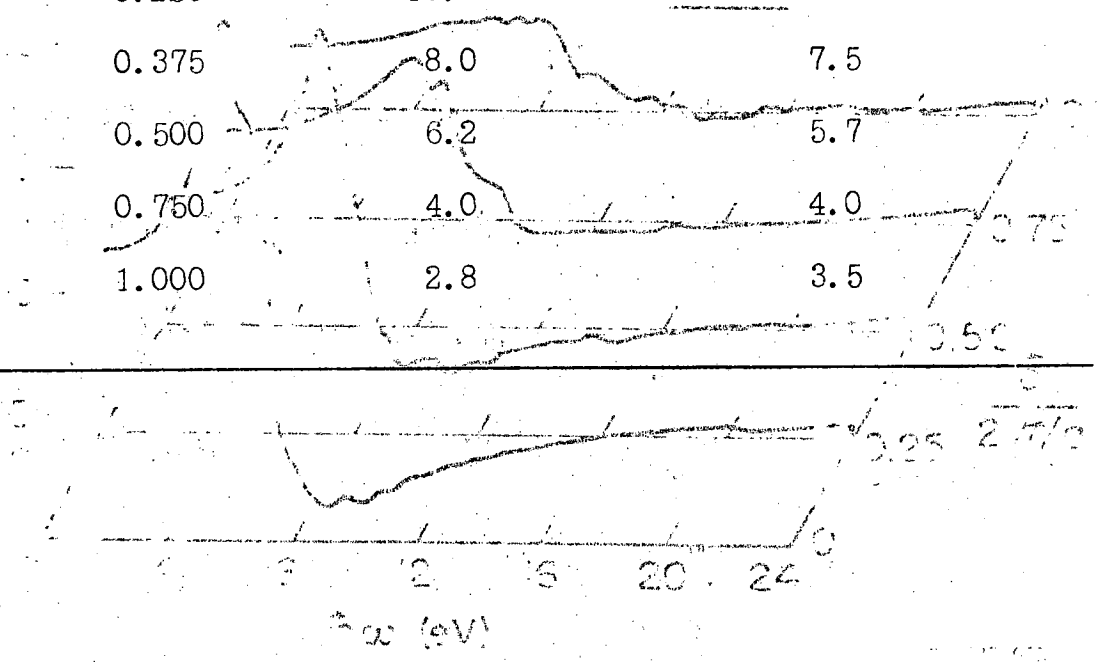

Fig. 2.

0 0 0 0 3 8 0 4 8 1 3

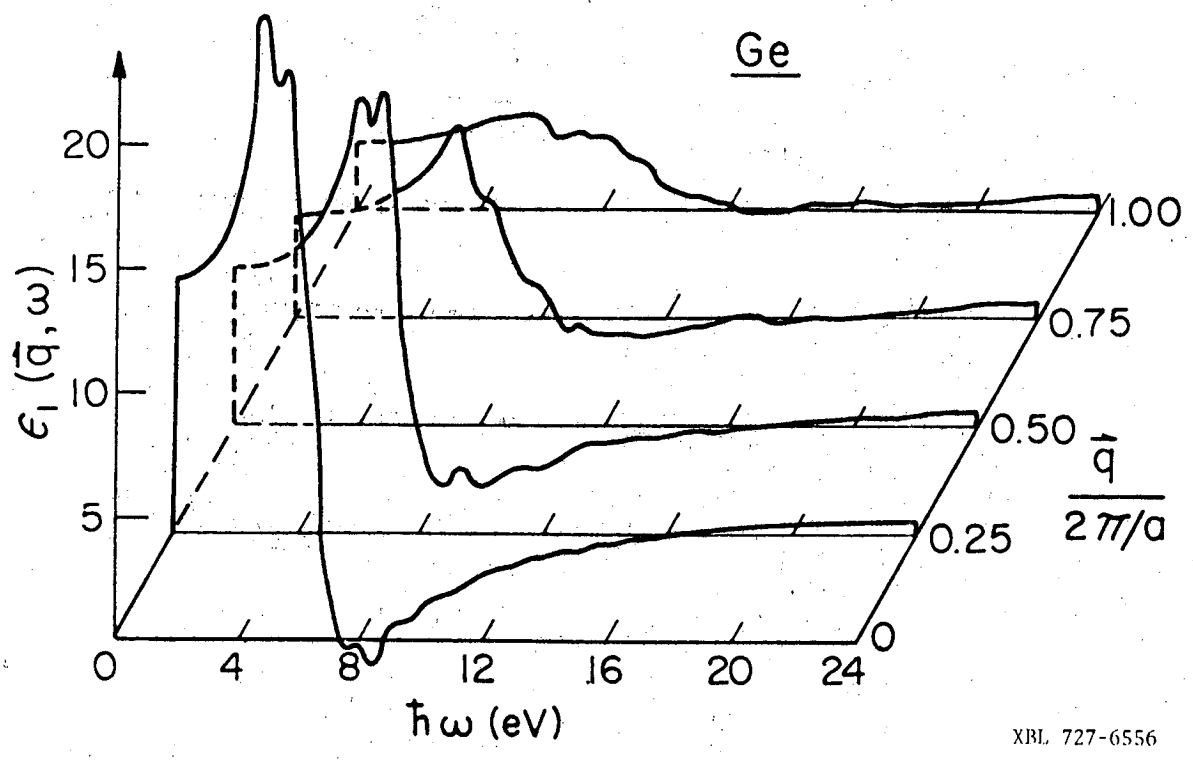

Fig. 1.

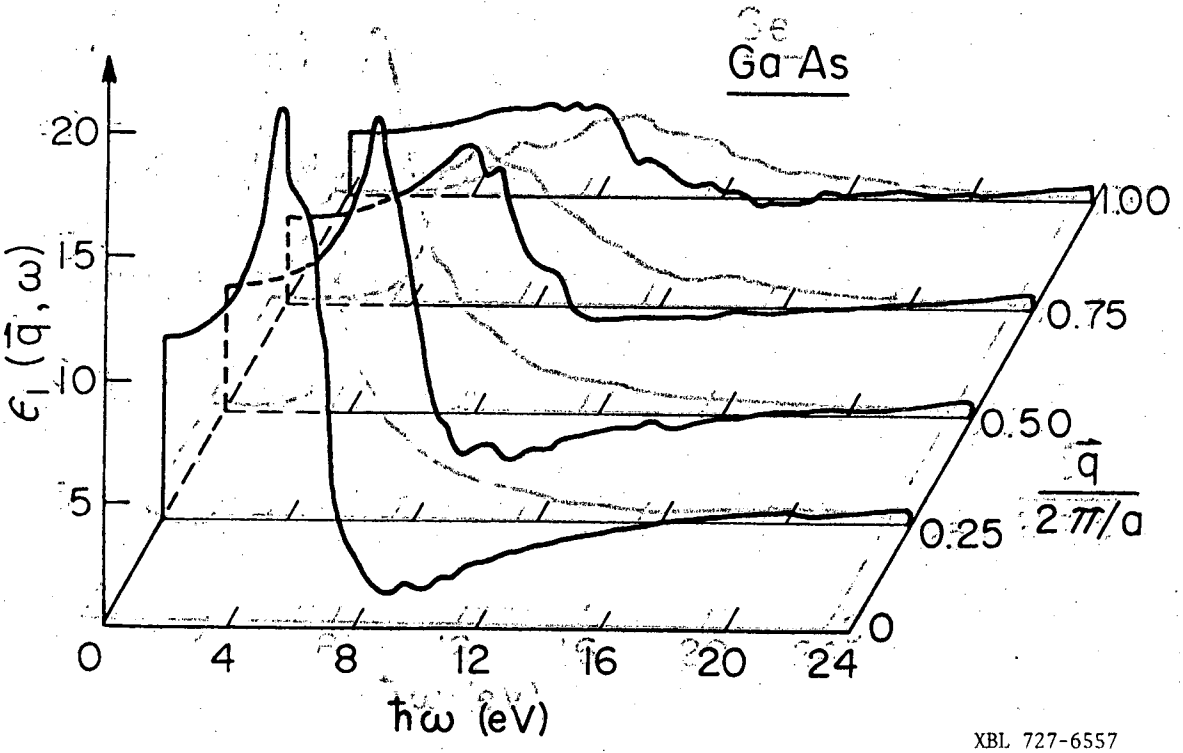
Ge
Ga As
20
15
10
5
$\epsilon_1(\vec{q},\omega)$
0
4
8
12
16
20
24
$\hbar\omega$ (eV)
1.00
0.75
0.50
0.25
0
$\frac{\vec{q}}{2\pi/a}$
XBL 727-6557

Fig. 2.

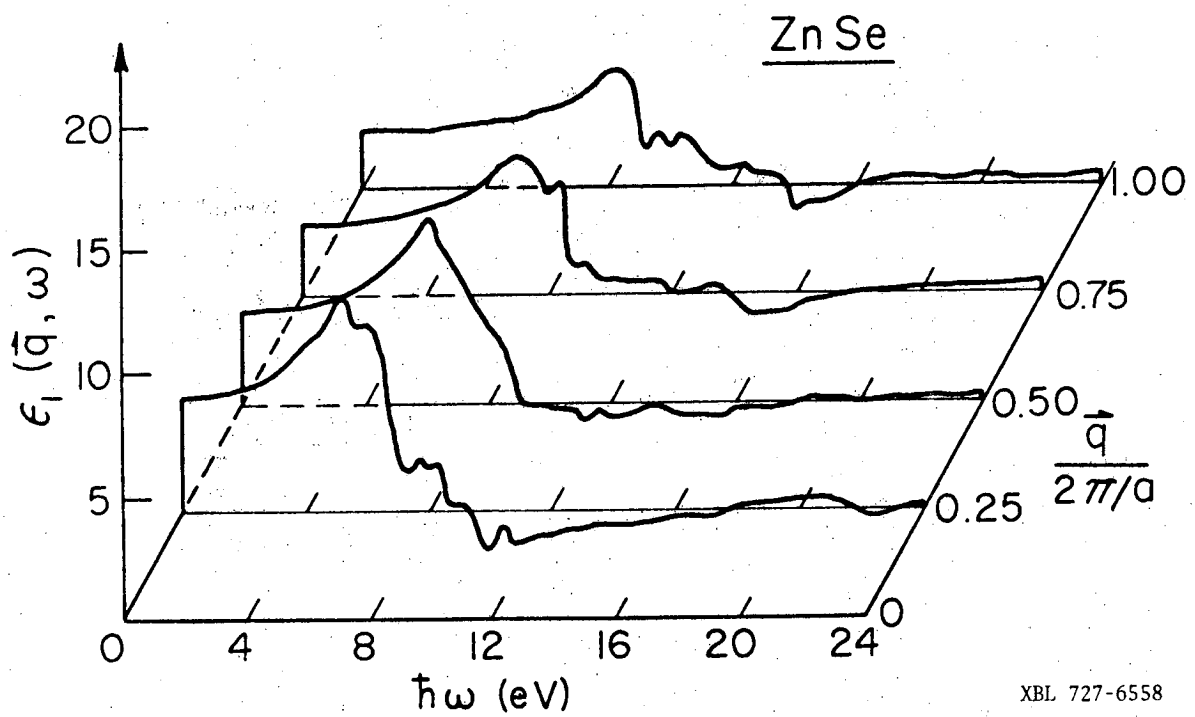
Zn Se
20
15
10
5
$\epsilon_1(\vec{q},\omega)$
0
4
8
12
16
20
24
$\hbar\omega$ (eV)
1.00
0.75
0.50
0.25
0
$\frac{\vec{q}}{2\pi/a}$
XBL 727-6558

Fig. 3.

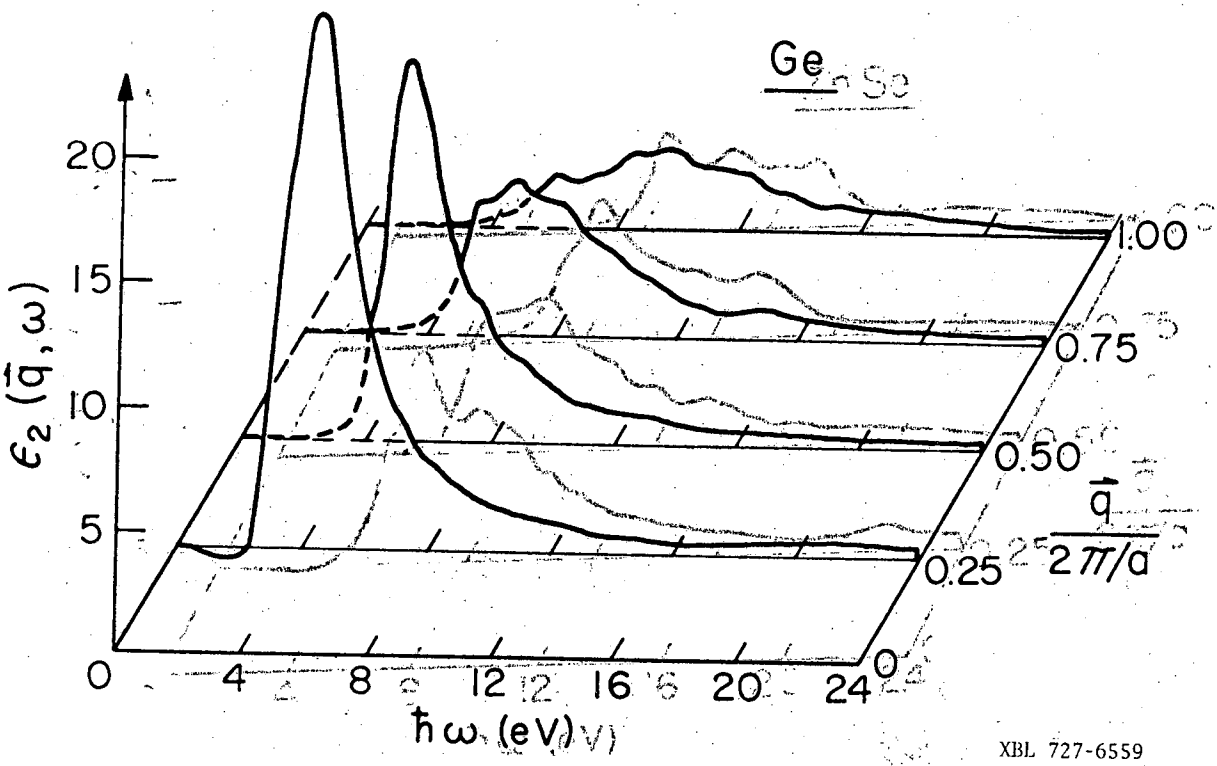
Ge
20
15
10
5
0
$\epsilon_2(\vec{q},\omega)$
4
8
12
16
20
24
$\hbar\omega$ (eV)
1.00
0.75
0.50
0.25
0
$\frac{\vec{q}}{2\pi/a}$
XBL 727-6559

Fig. 4.6.

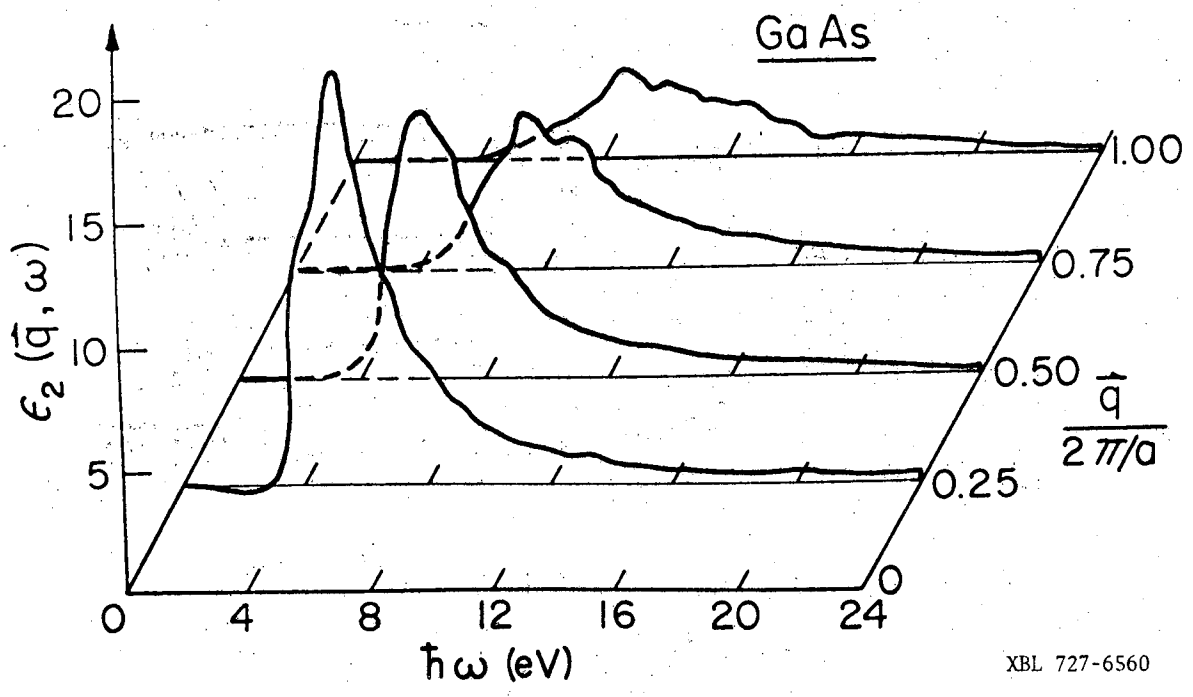
Ga As
20
15
10
5
0
$\epsilon_2(\vec{q},\omega)$
4
8
12
16
20
24
$\hbar\omega$ (eV)
1.00
0.75
0.50
0.25
0
$\frac{\vec{q}}{2\pi/a}$
XBL 727-6560

Fig. 5.

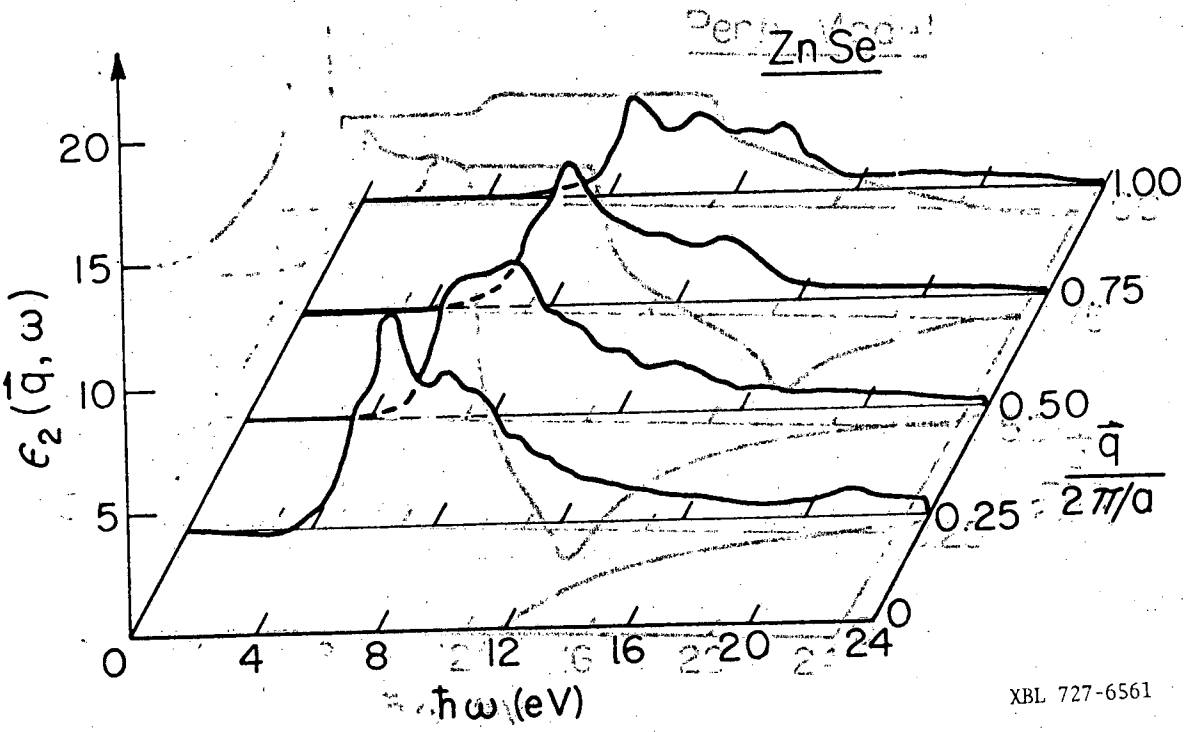
ZnSe
20
15
10
5
0
$\epsilon_2(\vec{q},\omega)$
4
8
12
16
20
24
$\hbar\omega$ (eV)
1.00
0.75
0.50
0.25
0
$\frac{\vec{q}}{2\pi/a}$
XBL 727-6561

Fig. 6.

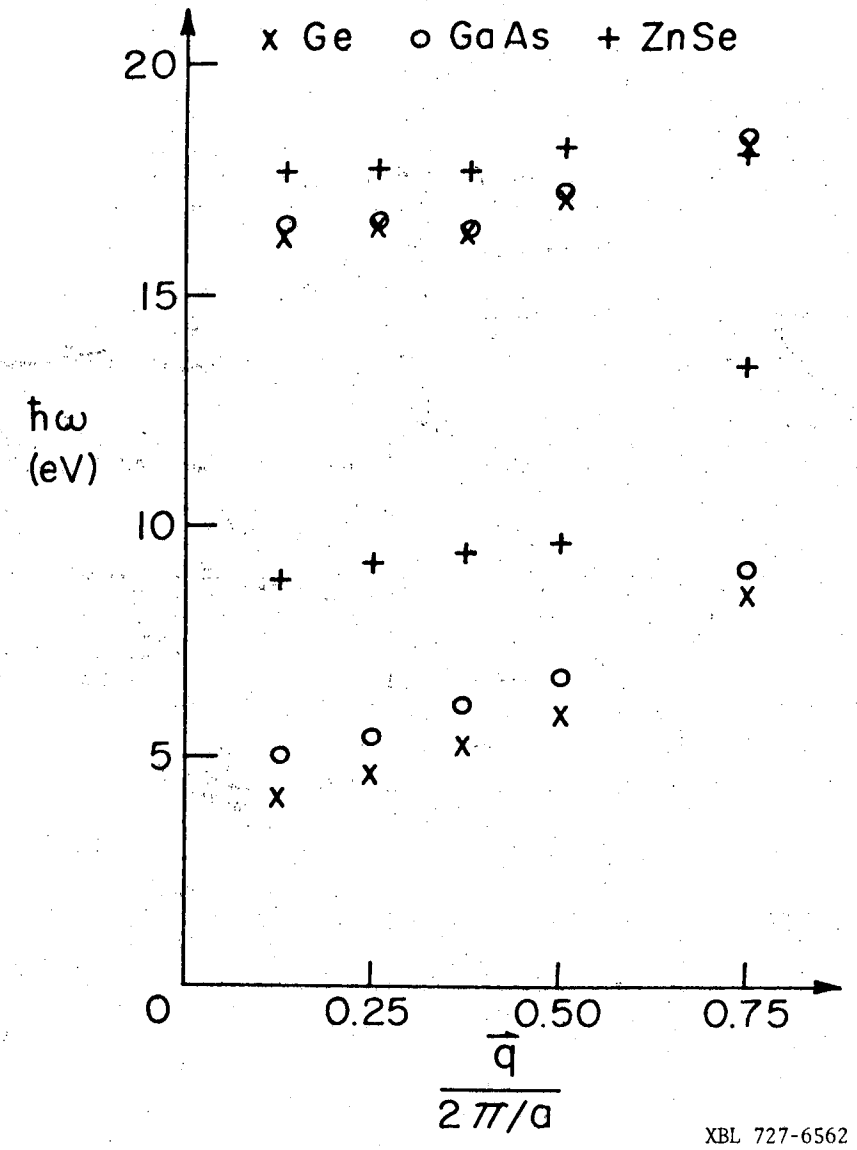

Fig. 7.

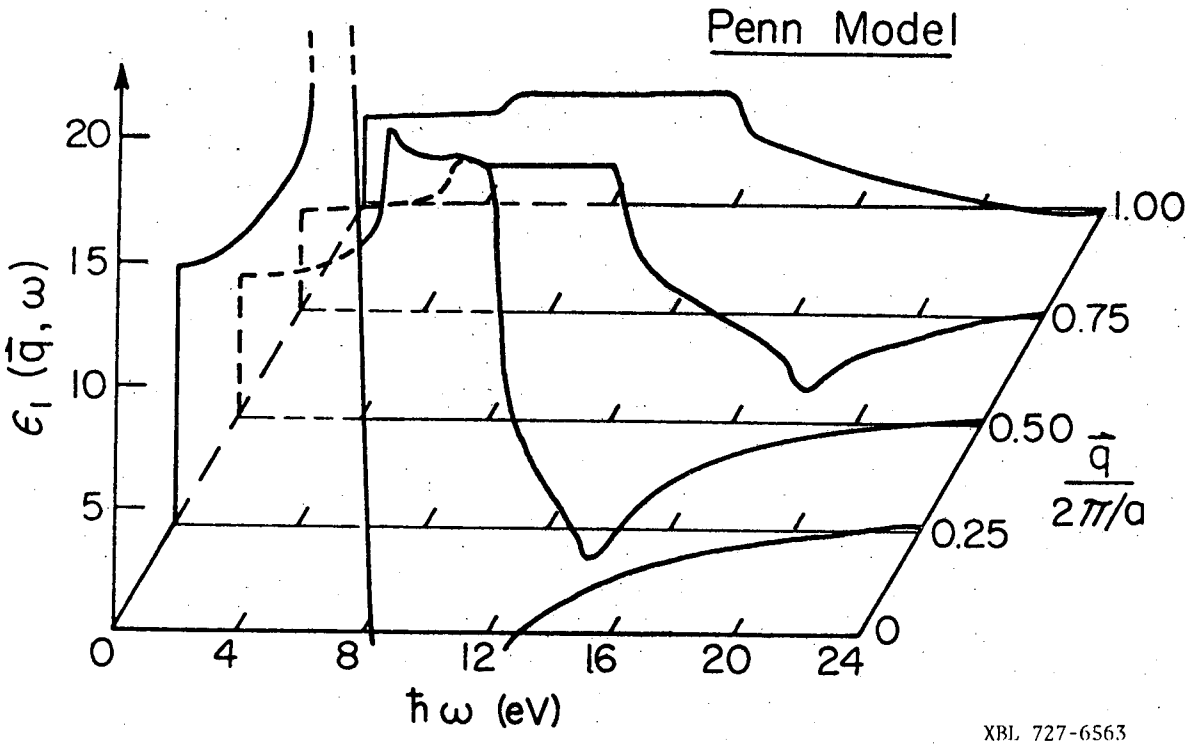
Penn Model
$\epsilon_1(\vec{q},\omega)$
20
15
10
5
0
4
8
12
16
20
24
$\hbar\omega$ (eV)
1.00
0.75
0.50
0.25
0
$\frac{\vec{q}}{2\pi/a}$
XBL 727-6563

Fig. 8.

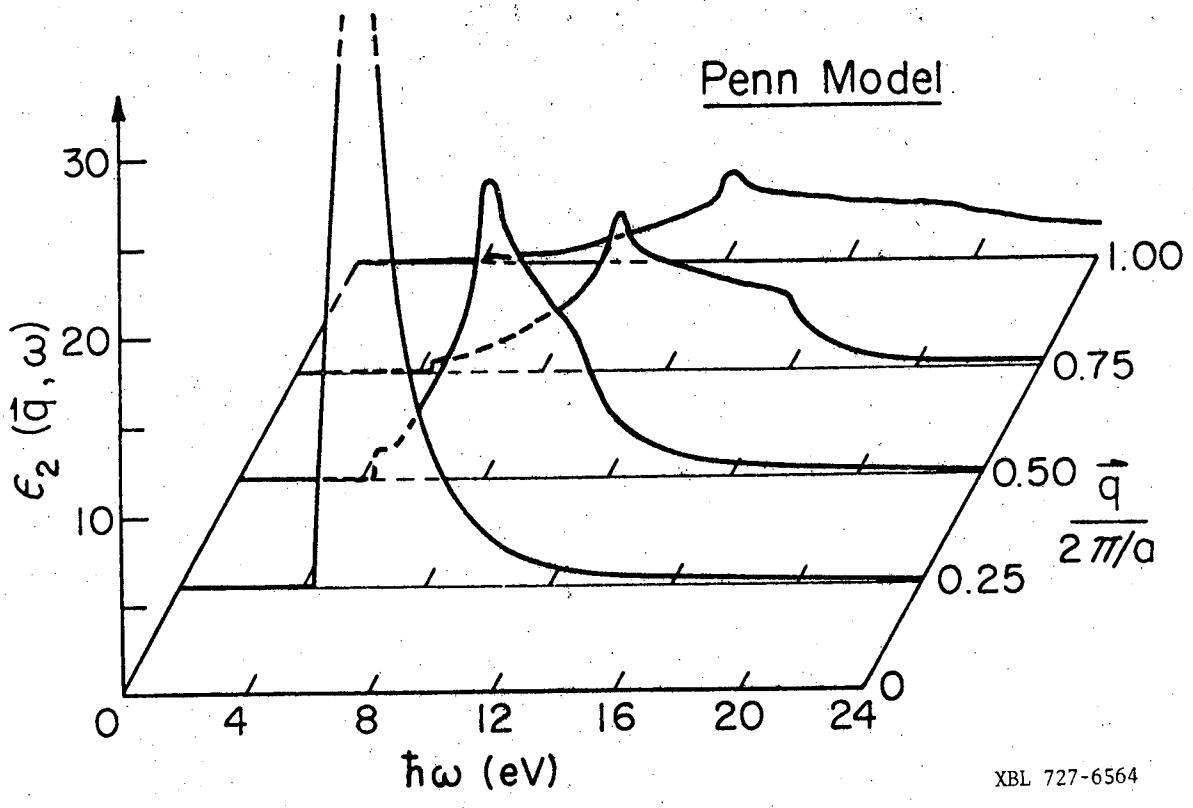
Penn Model
30
20
10
0
$\epsilon_2(\vec{q},\omega)$
0
4
8
12
16
20
24
$\hbar\omega$ (eV)
1.00
0.75
0.50
0.25
0
$\frac{\vec{q}}{2\pi/a}$
XBL 727-6564

Fig. 9.

LEGAL NOTICE

This report was prepared as an account of work sponsored by the United States Government. Neither the United States nor the United States Atomic Energy Commission, nor any of their employees, nor any of their contractors, subcontractors, or their employees, makes any warranty, express or implied, or assumes any legal liability or responsibility for the accuracy, completeness or usefulness of any information, apparatus, product or process disclosed, or represents that its use would not infringe privately owned rights.

TECHNICAL INFORMATION DIVISION
LAWRENCE BERKELEY LABORATORY
UNIVERSITY OF CALIFORNIA
BERKELEY, CALIFORNIA 94720